Journal of Power Sources 196 (2011) 8651–8655

Contents lists available at ScienceDirect

Journal of Power Sources

journal homepage: www.elsevier.com/locate/jpowsour

An inorganic membrane as a separator for lithium-ion battery

Hongfa Xiang, Jingjuan Chen, Zhong Li, Haihui Wang*

School of Chemistry & Chemical Engineering, South China University of Technology, Guangzhou 510641, Guangdong, China

ARTICLE INFO

Article history:
Received 18 March 2011
Received in revised form 4 May 2011
Accepted 15 June 2011
Available online 22 June 2011

Keywords:
Inorganic separator
Aluminum oxide
Lithium-ion battery

ABSTRACT

An Al_2O_3 inorganic separator is prepared by a double sintering process. The Al_2O_3 separator has a high porosity and good mechanical strength. After the liquid electrolyte is infiltrated, the separator exhibits quite high ionic conductivities, and even the conductivity reaches 0.78 mS cm^{-1} at −20 °C. Furthermore, the inorganic separator has an advantage over the polymer separator in the electrolyte retention. The $LiFePO_4$/graphite cell using the Al_2O_3 inorganic separator shows higher discharge capacity and rate capability, and better low-temperature performance than that using the commercial polymer separator, which indicates that the Al_2O_3 separator is very promising to be applied in the lithium-ion batteries.

1. Introduction

With fossil energy decreasing, the energy storage and conversion devices will play an increasing role in the future. Lithium-ion batteries are the most attractive secondary battery technology owing to their high energy density, long cycling lifetime and low self-discharge rate [1]. However, there are still some issues restricting the development of the lithium-ion batteries. High rate capability, long-term stability and high-temperature performances are strongly driven by the requirement of large-sized batteries for electric vehicles and long-term energy storage devices. Polymer separators made from polyolefins and polymer matrices in the gel electrolytes have been widely used in the commercial lithium-ion batteries. However, these organic materials usually have low melting points and poor mechanical strengths so that they could undergo obvious dimensional changes at elevated temperatures (∼100 °C) or be easily punctured by lithium dendrite commonly formed at high rates or long-term cycling [2,3]. Therefore, the organic separator could lead to some potential safety issues.

Inorganic materials have been widely used to modify the polymer separator due to their excellent thermal stability and electrolyte wettability [4–7]. These polymer separators modified by inorganic materials exhibit improved thermal properties and cell performances. Recently, the inorganic composite separators containing inorganic ceramic powders as the main component and organic materials have been developed to further improve the thermal stability of the batteries [8,9]. On the other hand, an inorganic solid electrolyte can act as both the separator and the electrolyte was also reported, but it is quite difficult for the solid electrolyte to sufficiently contact with the solid electrode owing to the absence of liquid electrolyte [10]. Purely inorganic separators have not been reported because of their poor flexibility for cell winding assembly. However, an inorganic separator plate can be available and attractive for the large-sized lithium-ion batteries in prismatic cell design or the other rigid battery designs [11]. Compared with the commercial polymer separator, the inorganic separator could have the advantages of “absolutely” thermal stability, strong electrolyte absorption and no dendrite puncturing problems. The safety characteristic of the inorganic separator makes it possible to constitute a large-sized single cell, which has obvious advantages over the battery pack consisting of many small cells. In addition, the purely inorganic separator could also be used for the attractive three-dimensional (3D) battery designs [12]. Although the potential applications of purely inorganic separators are extensive, many challenges limit their applications in the lithium-ion batteries. Besides the poor flexibility mentioned above, another obstacle is to prepare the thin separator with high porosity and good mechanical strength. In this paper, Al_2O_3 separator is prepared by a double sintering process. The as-prepared Al_2O_3 separator has sufficient strength for the cell assembly and high porosity for adsorbing enough electrolyte to get high conductivities and satisfactory cell performances. The electrochemical performances of the $LiFePO_4$/graphite cells using the as-prepared Al_2O_3 separator are investigated for the first time.

* Corresponding author. Tel.: +86 20 87110131; fax: +86 20 87110131.
E-mail address: hhwang@scut.edu.cn (H. Wang).

0378-7753/$ – see front matter © 2011 Elsevier B.V. All rights reserved.
doi:10.1016/j.jpowsour.2011.06.055

2. Experimental

2.1. Preparation of Al_2O_3 inorganic separators

The Al_2O_3 inorganic separators were prepared by a double sintering process as follows. First, neutral activated alumina (300 mesh), nano-sized Al_2O_3 powder (Qingdao Xinhai Ltd. Co.) and ethylenediaminetetraacetic acid (EDTA) as a pore-forming agent were mixed at the mass ratio of 3:3:4. Platelets (Φ16 mm) were pressed at a pressure of 10 Mbar and sintered at 1000 °C for 5 h in air. Porous Al_2O_3 platelets were formed by removing EDTA after sintering at 1000 °C. Then the sintered porous platelets were rinsed and ultrasonicated in ethanol for 5 min to remove some separated particles from the pores. After being dried in a vacuum oven for 12 h, the sintered porous Al_2O_3 platelets were re-sintered at 1500 °C for 5 h to get the final inorganic separators. The purpose of the first sintering was mainly to form the pores, but the mechanical strength of the plate is quite poor. After the re-sintering process at 1500 °C, the mechanical strength of the porous Al_2O_3 plates was significantly improved.

2.2. Physical and electrochemical measurements of the separators

The morphology of the Al_2O_3 separator was observed by scanning electron microscopy (SEM, LEO 1530 VP). The ionic conductivities of the Al_2O_3 separator infiltrated with the electrolyte solution of 1 M $LiPF_6$/EC + DEC (1:1, w/w) were measured by an electrochemical impedance spectroscopy (EIS) method. For the testing, the cells were formed by sandwiching the electrolyte-infiltrated Al_2O_3 separator between two stainless steel electrodes. The impedance measurements were carried out on an electrochemical workstation (Zahner IM6ex) in the frequency range from 10 mHz to 1 MHz with the potential perturbation of 10 mV. The ionic conductivities of the electrolyte of 1 M $LiPF_6$/EC + DEC (1:1, w/w) were measured over the temperature range of −20 to 60 °C using a Model DDS-307A conductometer (Shanghai Precision & Scientific Instrument Co. Ltd.). The temperature was controlled by a WD4005 low-temperature chamber (Xianchen Environment & Experimental Equipment Co. Ltd.). Each conductivity measurement was carried out after the electrolyte solution or the testing cells were held at a given temperature for 1 h in order to reach full thermal equilibration.

Electrolyte retention of the separator was evaluated as follows. At first, the initial weight (W_0) of the separator was measured before the separator was soaked in the electrolyte solution for 1 h. Then, the separator was taken out and the excrescent solution on the surface was absorbed with a filter paper. Subsequently, the electrolyte-infiltrated separator was weighed (W_1) again. Finally the separator was stored at 50 °C. The weight (W_x) of the separator was recorded at some interval. Typically, the electrolyte uptake and retention of the separator are calculated by the following equations [13]:

$$\text{Electrolyte uptake} = \frac{W_1 - W_0}{W_0} \times 100\% \quad (1)$$

$$\text{Electrolyte retention} = \frac{W_x - W_0}{W_1 - W_0} \times 100\% \quad (2)$$

where W_0 is the weight of separator, W_1 and W_x are the initial and equilibrium weights of the separator after absorbing the electrolyte solution, respectively. Three parallel measurements were carried out for either separator under the same conditions.

2.3. Cell performance measurements

A graphite electrode consisting of 90 wt% graphite (Hitachi Powdered Metals Co. Ltd.) and 10 wt% poly(vinylidene fluoride) (PVDF) and a positive electrode consisting of 80 wt% $LiFePO_4$ (Tianjin STL Co. Ltd.), 10 wt% acetylene black and 10 wt% PVDF were made on copper foils and aluminum foils, respectively. The mass loading of graphite and $LiFePO_4$ in the composite electrodes above was controlled at about 1.15 mg cm^{-2} and 2.65 mg cm^{-2}, respectively. The specific capacity of the $LiFePO_4$/graphite cells was calculated on the mass of $LiFePO_4$. CR2032 coin cells containing the $LiFePO_4$ positive electrode, the graphite negative electrode, and the inorganic separator infiltrated with the electrolyte of 1 M $LiPF_6$/EC + DEC (1:1), were assembled in an argon-filled glove box (Mikrouna). For comparison, the corresponding cells using the polymer separator (Celgard 2400) were also assembled and tested at the same conditions.

Charge–discharge cycle tests were performed at indicated current densities in the voltage range from 2.4 to 4.3 V using a NEWARE Battery Testing System. For the rate capability measurements, all the cells were charged to 4.3 V at 0.5 C and discharged to 2.4 V at different current rates at room temperature. Herein, 0.1 C means that it takes 10 h for the cell to drain in a predefined voltage window, and the corresponding current density is 0.033 mA cm^{-2}. Higher rate was set by adjusting the current density, e.g., 1 C was corresponding to the current density of 0.33 mA cm^{-2}. For the measurement of the low-temperature performance, all the cells were charged to 4.3 V at a rate of 0.2 C at room temperature. Then they were transferred into a low-temperature chamber and held for 30 min for heat equilibrium, followed by being discharged to 2.4 V at 0.2 C at the indicated temperature. The ac impedance was also measured on the Zahner IM6ex electrochemical workstation, with the frequency range and voltage amplitude set as 1 MHz to 0.01 Hz and 10 mV, respectively. Before the ac impedance measurements, the cells were cycled twice at 0.1 C and subsequently charged to 50% of the full capacity, the state of charge SOC = 50%.

3. Results and discussion

In lithium-ion batteries, the main function of separator is to prevent the positive and negative electrodes contacting and simultaneously allow rapid transport of lithium ions. Therefore, the separator should be a good electronic insulator and have the capability of conducting ions by soaking electrolyte. Porosity of the separator is one of the key parameters that determine high conductivity of the separator infiltrated with the electrolyte. However, inorganic separator with high porosity usually is extremely brittle for the cell assembly. It is difficult to fabricate the porous inorganic separator with satisfying mechanical strength. Herein, the Al_2O_3 inorganic separator was prepared by a double sintering method from the mixture of micron-sized Al_2O_3, nano-sized Al_2O_3 and EDTA. Fig. 1 shows the photographs and SEM images of the as-prepared Al_2O_3 separator. From Fig. 1a and b, the Al_2O_3 separator has a good surface integrity with a larger thickness (200 μm) than the polymer separator (25 μm). The SEM images indicate that the Al_2O_3 particles with the size of 200–500 nm have been successfully sintered, while the clear and homogeneous pores with the size of several hundred nanometers are formed. The porosity of the Al_2O_3 separator is also estimated to be around 70% based on the geometrical volume of the separator plate and the actual volume of the solid (the ratio of mass and the density of ∼4 g cm^{-3}), which is much higher than that of polymer separators (∼40%) [3]. Although the porosity of 70% is quite high, the separator still has sufficient mechanical strength owing to the solid bonding caused by re-sintering at 1500 °C. Furthermore, the combination of micron-

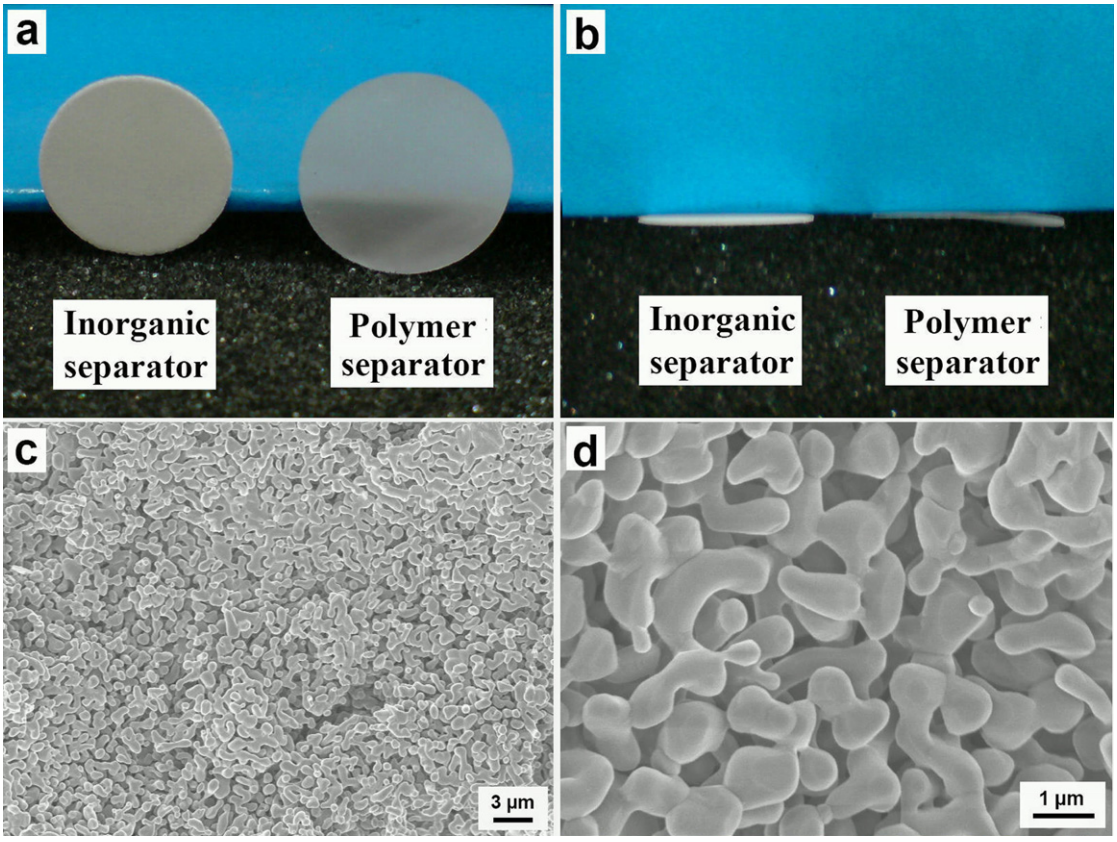

Fig. 1. Photographs (a and b) and SEM images (c and d) of the Al_2O_3 inorganic separator, compared with the commercial polymer separator.

sized and nano-sized Al_2O_3 is beneficial to both the high porosity and good mechanical strength. We also found that the mechanical strength of the Al_2O_3 separator is too poor to be used for the cell assembly if the nano-sized Al_2O_3 is absence or only in low content. The possible reason is that the nano-sized Al_2O_3 particles can be sintered more easily to form the solid bonding than the micron-sized particles.

Fig. 2 shows that the comparison of the ionic conductivities of the Al_2O_3 separator and the polymer separator infiltrated with electrolyte, and the individual liquid electrolyte under different temperatures. The Al_2O_3 separator infiltrated with the electrolyte exhibits slightly lower ionic conductivities than the liquid electrolyte, but higher ionic conductivities than the polymer separator infiltrated with electrolyte. For the two separators infiltrated with electrolyte, the temperature dependence of the conductivity is similar to that for the individual liquid electrolyte. Herein, our results are comparative to the literature reported by Zhang et al. [8]. As they proposed, the ionic conductivity in the separator was entirely contributed by the liquid electrolyte immobilized in the pores of the separator, so the ionic conductivity of the electrolyte-infiltrated separator is closely associated with the porosity of the separator. At room temperature (20 °C), the Al_2O_3 separator infiltrated with the electrolyte has an ionic conductivity of 3.45 mS cm^{-1}. The ionic conductivity reaches 0.78 mS cm^{-1} even at −20 °C, which can still meet the demand for the usual use. Here the inorganic separator infiltrated with the electrolyte has much higher ionic conductivities than most of the gel electrolyte systems [14,15]. It means that the inorganic separator can be used in a wide range of temperature. Moreover, the ionic conductivities of the purely inorganic separator containing the electrolyte are also higher than those reported by Zhang and coworkers, which is consistent with their finding that ionic conductivity of the electrolyte-infiltrated separator can be significantly enhanced by reducing the content of the polymer binder [8]. The satisfactory ionic conductivity of the inorganic separator infiltrated with the electrolyte could be mainly attributed to its high porosity.

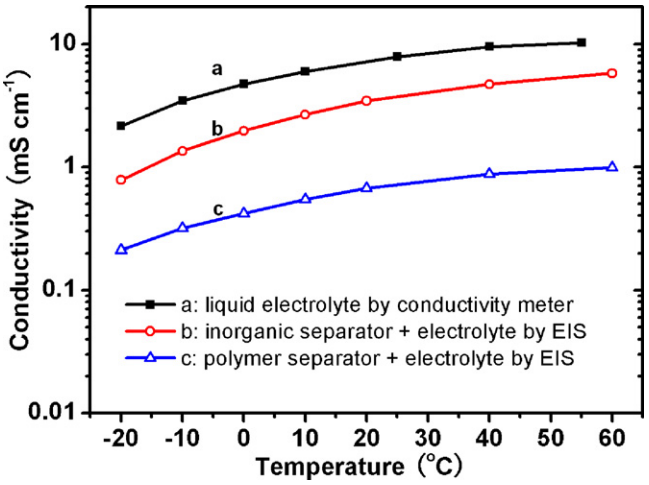

Fig. 2. Dependence of ion conductivity on temperature for the electrolyte-infiltrated inorganic separator and the polymer separator, and the electrolyte of 1 M $LiPF_6$/EC + DEC (1:1).

The electrolyte uptake of the separators has been investigated. Although the density of Al_2O_3 (~4 g cm^{-3}) is much higher than that of the polymer (e.g. ~0.9 g cm^{-3} of polypropylene in Celgard 2400), the electrolyte uptakes of the inorganic separator and the polymer separator are 200% and 230%, respectively. It means that the inorganic separator can adsorb much more electrolyte than the polymer separator with the same volume. The Al_2O_3 separator has more electrolyte absorption, possibly due to the stronger

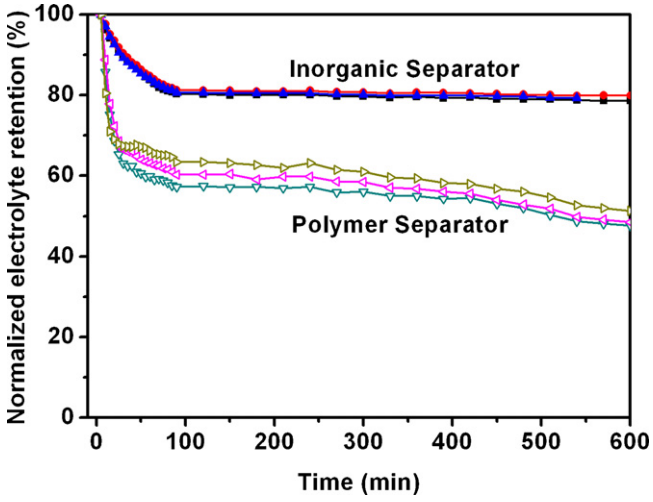

Fig. 3. Time dependence of the electrolyte retention of the Al_2O_3 inorganic separator and the polymer separator at 50 °C.

affinity of hydrophilic Al_2O_3 particles toward solvent molecules [16,17]. The affinity between Al_2O_3 and the electrolyte is also illustrated based on the electrolyte retention of the separator. The time dependence of the normalized electrolyte retention of the separators at 50 °C was shown in Fig. 3. It is found that the infiltrated electrolytes into the Al_2O_3 inorganic separator and the polymer separator are both reduced greatly at the beginning. After 100 min, the electrolyte retentions are 80% for the Al_2O_3 separator and ~60% for the polymer separator, respectively. Moreover, after 600 min, the electrolyte infiltrated in the polymer separator was reduced to only 50%, while no electrolyte loss was found in the Al_2O_3 separator during the period from 100 min to 600 min. The excellent electrolyte retention of the Al_2O_3 separator is mainly attributed to the following two reasons. One is the strong affinity of Al_2O_3 particles toward solvent molecules. The other is the capillary force due to the existence of many micropores in the Al_2O_3 separator.

Fig. 4 shows the initial voltage profiles and the cycling performance of the $LiFePO_4$/graphite full-cells using the Al_2O_3 inorganic separator and the commercial polymer separator. In Fig. 4a, the cell using the polymer separator has an initial discharge capacity of 121.5 mAh g^{-1} with a coulombic efficiency of 75.6%. However, the cell using the inorganic separator exhibits an initial discharge capacity of 127.2 mAh g^{-1} with the coulombic efficiency of 77.9%. The cycling performances of both cells (Fig. 4b) are quite good. The cell using the inorganic separator always has the higher discharge capacity than that using the polymer separator. In the first cycle, the low coulombic efficiency is commonly attributed to the formation of the solid electrolyte interface (SEI) layer. After two cycles, coulombic efficiencies of the both cells keep a quite high level close to 100%. One of the possible reasons for the improvement on the cell performances, especially the coulombic efficiency, is the reduced side reactions, since Al_2O_3 can capture the trace amounts of moisture and acidic impurity in the electrolyte [16].

The rate capability and the low-temperature performance of the $LiFePO_4$/graphite full-cells using the inorganic separator and the polymer separator are investigated further. The discharge voltage profiles of the cells using inorganic separator and the commercial polymer separator at different current rates are shown in Fig. 5. We can clearly see that the discharge voltage plateau drops with increasing the current rate for both the cells. But the cell using the inorganic separator always exhibits a higher discharge capacity than that using the polymer separator at the same current rate. At 0.5 C, the discharge capacities of the cells using the inorganic separator and the polymer separator are 124.0 and 108.8 mAh g^{-1},

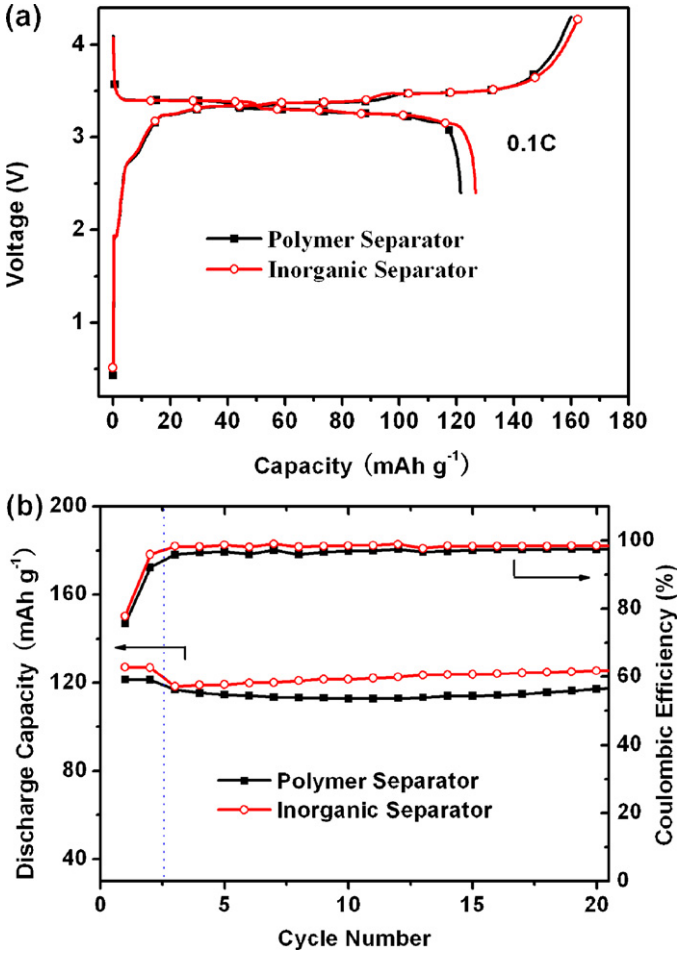

Fig. 4. Initial voltage profiles (a) and cycling performance (b) of the $LiFePO_4$/graphite cells using the Al_2O_3 inorganic separator and the polymer separator.

respectively. When the current rate is 6 C, the discharge capacities of the cells using the inorganic separator and the polymer separator are 82.8 and 70.9 mAh g^{-1}, respectively. Fig. 6 shows the comparison results of the cells using the inorganic separator and the polymer separator at low temperatures. For the cell using the polymer separator, the discharge capacities are 90.4 mAh g^{-1} at 0 °C and 50.1 mAh g^{-1} at −20 °C. However, for the cell using the inorganic

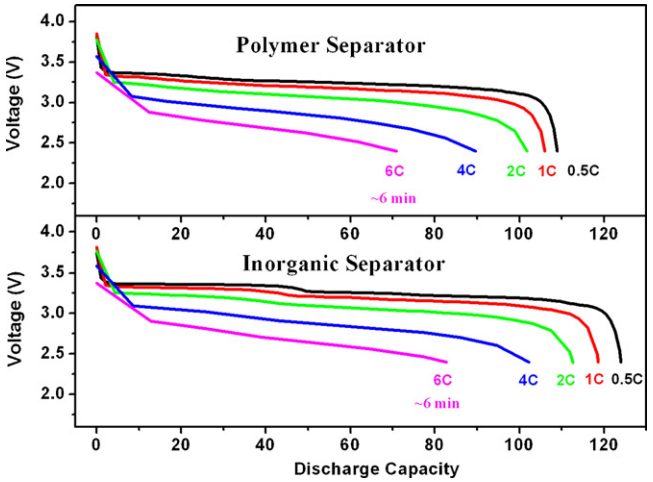

Fig. 5. Rate capability of the $LiFePO_4$/graphite cells using the Al_2O_3 inorganic separator and the polymer separator.

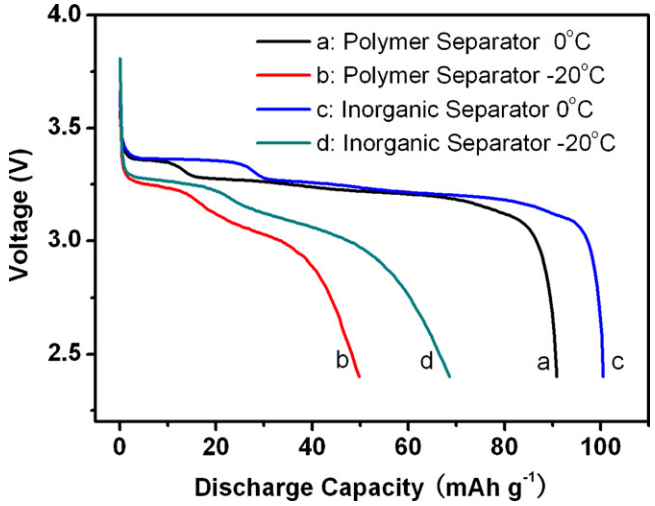

Fig. 6. Discharge curves of the $LiFePO_4$/graphite cells using the Al_2O_3 inorganic separator and the polymer separator at low temperatures.

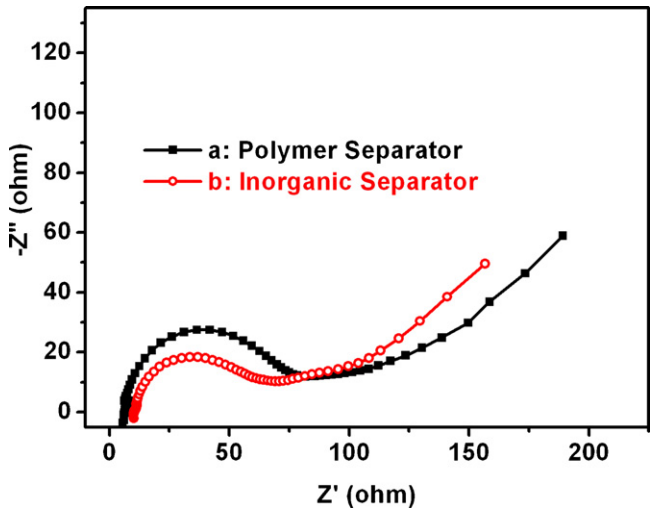

Fig. 7. Ac impedance spectra of the $LiFePO_4$/graphite cells using the Al_2O_3 inorganic separator and the polymer separator.

separator, the discharge capacities increase to 100.5 mAh g^{-1} at 0 °C and 69.2 mAh g^{-1} at −20 °C, respectively. As far as the capacity retention at low temperature is concerned, the discharge capacities of the cells using the inorganic separator and the commercial separator at −20 °C are 69% and 55% of the corresponding capacities at 0 °C, respectively. Therefore, the low-temperature performance of the $LiFePO_4$/graphite full-cell can be significantly improved by replacing the polymer separator with the inorganic separator.

The improved cell performance of the cell using the inorganic separator could be mainly attributed to the following reasons. Firstly, the capacity loss can be reduced, since Al_2O_3 can capture the trace amounts of moisture and acidic impurity in the electrolyte [16,18]. Therefore, the reversible capacity is increased. Secondly, the inorganic separator could indirectly contribute to reduced resistance of the cell. Although the ionic resistance has not been reduced directly, the whole resistance of the cell still could decrease indirectly, e.g., the SEI layer with lower resistance. This point has been validated by the ac impedance spectra, as shown in Fig. 7. Obviously, the cell using the inorganic separator has the reduced impedance of the SEI layer, which is indicated by the semicircle in the high-frequency region. Finally, it is seldom mentioned that lithium ion transfer number in the inorganic separator with strong affinity toward polar solvents or big-size ions PF_6^- could be enhanced, which should also improve the cell performance, especially the rate capability. In summary, the $LiFePO_4$/graphite full-cells using the inorganic separator exhibit better performances, including discharge capacity, rate capability and low-temperature performance than those using the polymer separator. The possible reasons are mainly attributed to the high porosity of the inorganic separator and the good affinity between the hydrophilic Al_2O_3 particles and the polar solvents. Moreover, Al_2O_3 can improve the interface layers between the electrodes and the electrolyte by capturing the trace amounts of moisture and acidic impurity in the electrolyte.

4. Conclusions

The Al_2O_3 inorganic separator with high porosity and good mechanical strength has been prepared by a double sintering process. The electrolyte-infiltrated Al_2O_3 separator exhibits an excellent ionic conductivity, and even at −20 °C its ionic conductivity reaches a utilizable level of 0.78 mS cm^{-1}. The $LiFePO_4$/graphite cell using the inorganic separator shows higher discharge capacity and rate capability, and better low-temperature performance than that using the commercial polymer separator. All the evidences indicate that the inorganic separator is very promising to be applied in the large-sized lithium-ion batteries, especially for the long-term energy storage systems. Moreover, after the inorganic separator is combined with some special electrolytes, e.g., ionic liquid based electrolytes with excellent thermal stability, it is possible to construct some special lithium-ion batteries that could be used in an extra-wide range of temperature from low temperature (e.g., −20 °C) to high temperature close to 300 °C in the future.

Acknowledgements

This work was supported by National Science Foundation of China (grant no. 21006033), China Postdoctoral Science Foundation, Program for New Century Excellent Talents in Chinese Ministry of Education (No. NECT-07-0307) and the Fundamental Research Funds for the Central Universities, SCUT (2009220038).

References

[1] J.M. Tarascon, M. Armand, Nature 414 (2001) 359.
[2] D. Aurbach, E. Zinigrad, H. Teller, P. Dan, J. Electrochem. Soc. 147 (2000) 1274.
[3] S.S. Zhang, J. Power Sources 164 (2007) 351.
[4] C.G. Wu, M.I. Lu, C.C. Tsai, H.J. Chuang, J. Power Sources 159 (2006) 295.
[5] H.S. Jeong, D.W. Kim, Y.U. Jeong, S.Y. Lee, J. Power Sources 195 (2010) 6116.
[6] M. Kim, G.Y. Han, K.J. Yoon, J.H. Park, J. Power Sources 195 (2010) 8302.
[7] Y.H. Liao, M.M. Rao, W.S. Li, L.T. Yang, B.K. Zhu, R. Xu, C.H. Fu, J. Membr. Sci. 352 (2010) 95.
[8] S.S. Zhang, K. Xu, T.R. Jow, J. Power Sources 140 (2005) 361.
[9] D. Takemura, S. Aihara, K. Hamano, M. Kise, T. Nishimura, H. Urushibata, H. Yoshiyasu, J. Power Sources 146 (2005) 779.
[10] J.B. Goodenough, Y. Kim, Chem. Mater. 22 (2010) 587.
[11] J.W. Fergus, J. Power Sources 195 (2010) 4554.
[12] J. Li, C. Daniel, D. Wood, J. Power Sources 196 (2011) 2452.
[13] C.G. Wu, M.I. Lu, H.J. Chuang, Polymer 46 (2005) 5929.
[14] W.L. Qiu, X.H. Ma, Q.H. Yang, Y.B. Fu, X.F. Zong, J. Power Sources 138 (2004) 245.
[15] X.M. He, Q. Shi, X. Zhou, C.R. Wan, C.Y. Jiang, Electrochim. Acta 51 (2005) 1069.
[16] Y.H. Liao, X.P. Li, C.H. Fu, R. Xu, L. Zhou, C.L. Tan, S.J. Hu, W.S. Li, J. Power Sources 196 (2011) 2115.
[17] J.A. Choi, S.H. Kim, D.W. Kim, J. Power Sources 195 (2010) 6192.
[18] Y.S. Lee, Y.B. Jeong, D.W. Kim, J. Power Sources 195 (2010) 6197.